Available at
www.ElsevierComputerScience.com
POWERED BY SCIENCE DIRECT®

Signal Processing 84 (2004) 881–894

SIGNAL PROCESSING

www.elsevier.com/locate/sigpro

Constant modulus blind equalization based on fractional lower-order statistics

Marilli Rupi[a], Panagiotis Tsakalides[b,*], Enrico Del Re[a], Chrysostomos L. Nikias[c]

[a] *Dipartimento di Ingegneria Elettronica, Universitá degli Studi di Firenze, I-50139 Firenze, Italy*
[b] *Institute of Computer Science, Foundation for Research and Technology-Hellas (FORTH), Department of Computer Science, University of Crete, 714 09 Heraklion, Greece*
[c] *Department of Electrical Engineering, University of Southern California, CA 90089-2561, USA*

Received 19 April 2002; received in revised form 23 December 2003

Abstract

The presence of non-Gaussian ambient channel noise in wireless systems can degrade the performance of existing equalizers and signal detectors. In this paper, we investigate the problem of blind equalization in noisy communication channels by addressing the negative effects of heavy-tailed noise to the original constant modulus algorithm (CMA). We propose a new CM criterion employing fractional lower-order statistics (FLOS) of the equalizer input. The associated FLOS-CM blind equalizer, based on a stochastic gradient descent algorithm, is able to mitigate impulsive channel noise while restoring the constant modulus character of the transmitted communication signal. We perform an analytic study of the lock and capture properties of the proposed adaptive filter and we illustrate its improved convergence behavior and lower bit error rate through computer simulations with various types of noise environments that include the Gaussian and the alpha-stable.

Keywords: Impulsive interference; Stable processes; Adaptive blind equalization; Constant modulus criterion; Fractional lower-order statistics

1. Introduction

The rapidly increasing demand for personal mobile communications has created an avid interest in innovative services and in new robust signal processing techniques, which could better protect and recover the transmitted information sequence. Extensive research effort has been directed towards propagation impairment abatement and interference mitigation in order to make efficient use of the finite spectral resources of a physical channel.

The atmosphere and the ocean, playing the role of the physical channel in wireless communications, can cause signal distortion due to finite bandwidth and signal fading due to multipath propagation. Channel distortion results in intersymbol interference (ISI) that creates high error rates at the receiver. In addition, the radio channel characteristics are unknown a priori and they change with time. Hence, an equalizer must

* Corresponding author. Institute of Computer Science, Foundation for Research and Technology-Hellas (FORTH), Science and Technologic Park of Crete, Vassilika Vouton, P.O. Box 1385, GR-711 10 Heraklion, Crete, Greece. Tel.: +30-2810-391-730; fax: +30-2810-391-601.

E-mail addresses: marilli@lenst.die.unifi.it (M. Rupi), tsakalid@csd.uoc.gr, tsakalid@ics.forth.gr (P. Tsakalides), nikias@imsc.usc.edu (C.L. Nikias).

0165-1684/$ - see front matter © 2004 Elsevier B.V. All rights reserved.
doi:10.1016/j.sigpro.2004.01.006

be adjusted to the channel response in real time. In the past, an abundance of adaptive linear equalizers have been proposed, which optimize an appropriate performance index to adaptively compensate for the effects of the channel [12]. A large portion of the proposed methods assumes the availability of a training sequence at the receiver for the purpose of initially adjusting the equalizer coefficients. However, in applications such as multiuser communication networks and mobile communication systems, it is desirable for the receiver to be able to equalize the channel without the use of a training sequence (self-recovering or blind equalization) [6].

Sato's original work on PAM signals [16] and subsequently Godard's generalization on multi-dimensional signal constellations were the forerunners of present-day blind equalizers [5]. During the 1990s, a great interest in wireless communication applications including blind equalization, source separation, and antenna beamforming has driven research into the development of fast and robust algorithms. Nowadays, one of the most studied and implemented in practice blind equalization methods is the constant modulus algorithm (CMA). The CMA is based on a criterion that penalizes deviations of the modulus of the equalized signal away from a fixed value determined by the source alphabet. Strikingly, CMA has also been successful in equalizing sources not possessing a constant modulus property, such as QAM constellations. Hence, CMA is a method that may be applied over the majority of radio communication signals. The first major study of the CMA and its properties was performed by Treichler et al. [20,26] who analyzed the capture and lock behavior of baud-spaced CMA. Recently, a review paper by Johnson et al. [7] summarized the emerging literature on the CM criterion for blind fractionally spaced equalizer (FSE) design via a stochastic gradient descent algorithm.

The vast majority of initial studies in blind equalization in general and the CMA method in particular have considered noise-free channels since it was argued that ISI is the major reason for signal degradation. This argument might be valid in wired communication channels such as coaxial, fiber optic, or twisted-pair cable, but it does not always hold in wireless channels where the channel medium cannot be controlled as effectively. Lately, Fijalkow et al. [3] studied the effects of additive Gaussian channel noise to the FSE-CM cost function. They showed that the noisy FSE-CM cost function is subject to a smoothing effect with respect to the noise-free cost function, resulting in a tradeoff between zero-forcing gain and noise enhancement. They modeled the additive channel noise as Gaussian, temporally and spatially white.

By and large, the Gaussian distribution has been the favorite noise model commonly employed in radio communications mainly because it often leads to closed-form solutions and to linear processors. However, in wireless channels, multiuser interference, atmospheric noise (thunderstorms), car ignitions, and other types of naturally occurring or man-made signal sources result in an aggregate noise component that may exhibit high amplitudes for small duration time intervals [13,18]. Recent experimental measurements have demonstrated that the ambient channel noise is decidedly non-Gaussian due mostly to impulsive phenomena (see [25] and references therein). It has been shown that electromagnetic noise in urban mobile-radio channels is heavy-tailed in nature and can be better modeled by using distributions with algebraic tails rather than the Gaussian or other exponentially tailed distributions [9–11].

Detection and estimation algorithms designed under the Gaussian assumption exhibit various degrees of performance degradation, depending on the non-Gaussian nature of the noise. This is due to the lack of robustness of linear and quadratic types of signal processors to many sorts of non-Gaussian environments [8]. On the other hand, non-Gaussian noise may actually be beneficial to a system's performance if appropriately modeled and treated [25]. For this reason, engineers have recognized the need to use more general and realistic non-Gaussian models and design robust signal processing techniques that take into account the heavy-tail nature of the data.

Recently, a statistical model of heavy-tailed interference, based on the theory of alpha-stable random processes, has been proposed for signal processing applications [11]. The family of alpha-stable distributions arises under very general assumptions and describes a broad class of impulsive interference. It is a parsimonious statistical–physical model defined (in its most general form) by only four parameters that can be efficiently estimated directly from the data. Furthermore, the alpha-stable model is the only one whose members obey the stability property and the

generalized central limit theorem. For these and other reasons, explained in greater detail in Section 2, statisticians, economists, signal processing and communications engineers, and other scientists engaged in a variety of disciplines have embraced alpha-stable processes as the model of choice for heavy-tailed data [1].

In [14], we showed that the presence of heavy-tailed noise has a negative effect on the CMA performance in terms of its convergence behavior. In this paper, we propose a novel constant modulus algorithm to address the presence of noise that can be modeled according to the alpha-stable law. The new method is based on the constant modulus property of the fractional lower-order statistics of the signal of interest and is able to handle robustly heavy-tailed noise and interference in the data. In the absence of noise, the performance of the proposed method is comparable with that of the original CMA.

The paper is organized as follows: in Section 2, we give a brief overview on alpha-stable distributions and the associated fractional lower-order statistics. In Section 3.1, we summarize the standard CMA method while in Sections 3.2 and 3.3, we introduce the new CMA criterion and study its lock and capture behavior. In Section 4, we demonstrate the robustness of the new receiver when operating over noisy channels of a heavy-tailed nature. In Section 5, we summarize the main results and we present avenues of future research.

2. A model for heavy-tailed interference

Heavy-tailed distributions and processes have been used in the past to analyze data that cannot be appropriately modeled by the Gaussian density [1,11]. Recently, a particular class of heavy-tailed distributions, namely the alpha-stable family, has been used to describe phenomena encountered in several communications applications. In computer networking, Taqqu et al. showed that file sizes and associated transmission times over the World Wide Web exhibit heavy-tails that can be described with the alpha-stable model [2]. Even more importantly for the purposes of this paper, the alpha-stable family has been shown to be an accurate statistical–physical model for heavy-tailed noise encountered in wireless communication channels. The stable model was derived from the familiar filtered-impulse mechanism of the noise process under

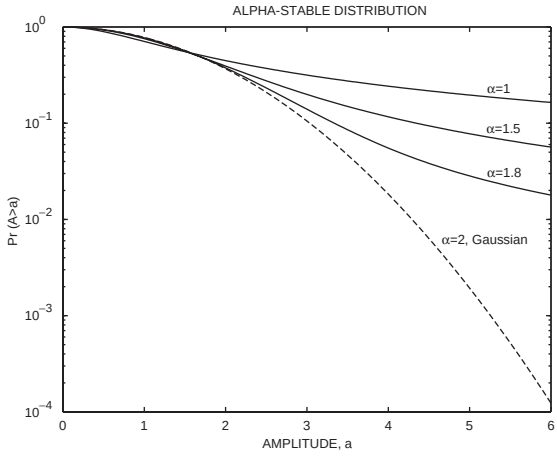

Fig. 1. Symmetric alpha-stable amplitude probability density functions ($\Pr(A > a)$). Dispersion is $\gamma = 1$ and characteristic exponent is $\alpha = 1.0$, 1.5, 1.8, and 2.0 (Gaussian).

appropriate assumptions on the spatial and temporal distributions of the noise sources and the propagation conditions to the receiver [11, Chapter 9].

The class of symmetric alpha-stable distributions is best defined by its characteristic function:

$$\varphi(\omega) = \exp(\mathrm{j}\delta\omega - \gamma|\omega|^{\alpha}), \tag{1}$$

where α is the *characteristic exponent* restricted to the values $0 < \alpha \leqslant 2$, $\delta(-\infty < \delta < \infty)$ is the *location parameter*, and $\gamma(\gamma > 0)$ is the *dispersion* of the distribution. The dispersion parameter γ determines the spread of the distribution around its location parameter δ. The characteristic exponent α determines the shape of the distribution (cf. Fig. 1). The smaller the characteristic exponent α is, the heavier the tails of the alpha-stable density. We should also note here that the stable distribution corresponding to $\alpha = 2$ coincides with the Gaussian density.

Alpha-stable densities obey two important properties which further justify their role in data modeling, namely (i) the *stability property*, which states that the weighted sum of independent alpha-stable random variables (r.v.'s) is stable with the same characteristic exponent alpha, and (ii) the *generalized central limit theorem* (GCLT), which states that stable models are the *only* distributions that can be the limit distributions of independent and identically distributed random variables. GCLT implies that if the observed randomness is the result of many cumulative effects

(as is the case in radio channels where the ambient noise is due to reflections from many scatterers) and these effects follow a heavy-tailed distribution, then a stable model may be appropriate.

An important difference between the Gaussian and the other distributions of the alpha-stable family is that only moments of order less than α exist for the non-Gaussian alpha-stable family members. The *fractional lower order moments* (FLOMs) of an alpha-stable random variable with zero location parameter and dispersion γ are given by

$$E|X|^p = C(p,\alpha)\gamma^{p/\alpha} \quad \text{for} \quad 0 < p < \alpha, \tag{2}$$

where $E[\cdot]$ denotes statistical expectation and $C(p,\alpha)$ is a constant depending only on p and α. Moreover, if $X_1,\ldots,X_n$ are dependent and jointly alpha-stable r.v.'s, then

$$E[|X_1|^{p_1}\cdots|X_n|^{p_n}] < \infty \tag{3}$$

if and only if $0 < p_1 + \cdots + p_n < \alpha$.

In the theory of second-order processes, the concepts of *variance* and *covariance* play the important roles of norms in problems of linear prediction, filtering and smoothing. Since non-Gaussian alpha-stable processes do not possess finite pth-order moments for $p \geqslant \alpha$, covariances do not exist on the space of alpha-stable random variables. For a zero location alpha-stable random variable X with dispersion γ, the *norm* of X is defined as

$$\|X\|_\alpha = \begin{cases} \gamma^{1/\alpha}, & 1 \leqslant \alpha \leqslant 2, \\ \gamma, & 0 < \alpha < 1. \end{cases} \tag{4}$$

Hence, the norm $\|X\|_\alpha$ is a scaled version of the dispersion γ. If X and Y are jointly alpha-stable, the distance between X and Y is defined as

$$d_\alpha(X,Y) = \|X - Y\|_\alpha. \tag{5}$$

Combining (2) and (4), it is easy to see that

$$d_\alpha(X,Y) = \begin{cases} (E(|X-Y|^p)/C(p,\alpha))^{1/p}, & 0 < p < \alpha, \\ & 1 \leqslant \alpha \leqslant 2, \\ (E(|X-Y|^p)/C(p,\alpha))^{\alpha/p}, & 0 < p < \alpha, \\ & 0 < \alpha < 1. \end{cases} \tag{6}$$

Thus, the pth-order moment of the difference between two alpha-stable random variables is a measure of the distance d_α between these two random variables. In the case of $\alpha = 2$ (Gaussian), this distance is half the variance of the difference. In addition, all fractional lower-order moments of an alpha-stable random variable are equivalent, i.e., the pth- and qth-order moments differ by a constant factor independent of the random variable as long as $p, q < \alpha$. Furthermore, it was shown by Schilder [17] that for $1 \leqslant \alpha \leqslant 2$, $\|\cdot\|_\alpha$ defined in (4) is a norm in the linear space of alpha-stable processes. Our proposed blind equalization methodology presented in the following section uses the notion of fractional lower-order moments to achieve robust noise suppression and signal recovery.

Compared with existing statistical models for ambient noise and interference, signal processing algorithms based on alpha-stable models for detection, parameter estimation, and array processing demonstrate robustness even in the presence of mismatches in the assumed conditions of noise and interference [11]. In addition, the use of fractional lower-order statistics is simple to understand and implement in real-time processing scenarios.

3. The FLOS-CM criterion for robust blind equalization

In this section, we first recall the original CMA to provide the necessary background and context before introducing our proposed method that is based on FLOS. In [14], we studied a FLOS-based fractionally spaced equalizer that exploited the spatial diversity at the receiver by combining the outputs of an array of sensors. More examples on important work on FSE using temporal and spatial diversity can be found in [3] and references therein. Although fractionally spaced equalizers have the ability to perfectly cancel ISI caused by a finite-length channel, in this paper we consider a baud-spaced (non-FSE) equalizer since our goal is to address and remedy the effects of ambient noise to the original CM criterion. Extension of our present work to FSE receivers is currently pursued by the authors.

3.1. The CM cost function

A multipath distorted communication signal is the input to the receiver shown in Fig. 2. The signal is

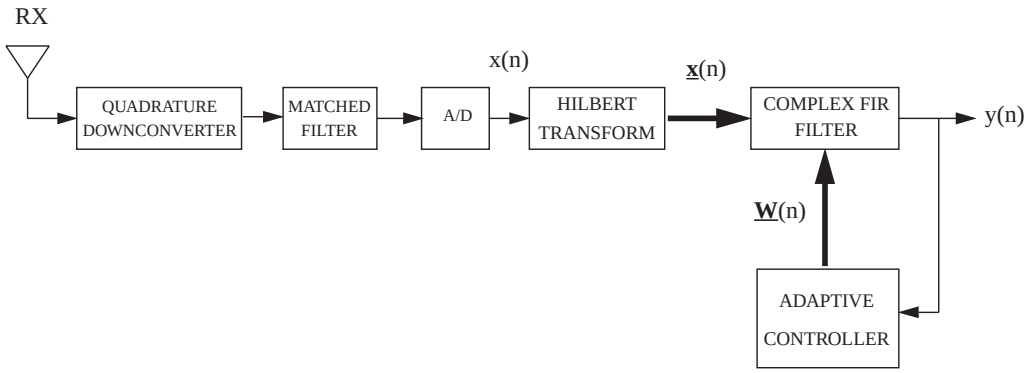

Fig. 2. FIR filter configuration employing the CMA.

down-converted to baseband, match filtered, Hilbert transformed into complex form, and sampled according to the Shannon theorem. The resulting signal $x(n)$ is applied to a finite impulse response filter with adjustable complex coefficients. We may write the complex equalizer output as

$$y(n) = \mathbf{x}^{\mathrm{t}}(n)\mathbf{w}(i), \tag{7}$$

where $\mathbf{x}(n)$ is the vector of data in the filter delay line,

$$\mathbf{x}(n) = [x(n)\ x(n-1)\cdots x(n-N+1)]^{\mathrm{t}} \tag{8}$$

and $\mathbf{w}(i)$ is the vector of adjustable coefficients, given by

$$\mathbf{w}(i) = [w_0(i)\ w_1(i)\cdots w_{N-1}(i)]^{\mathrm{t}}. \tag{9}$$

The index i indicates that the complex weights are adapted in time. Although not required, we assume that the adaptation time i is exactly the same as the sampling time n.

The CM adaptive equalizer tries to restore the constant envelope property of the communication signal, which is destroyed by frequency-selective multipath, additive noise, and suboptimal receiver bandpass filtering. The constant modulus cost function assigns a penalty to deviations in the modulus of the controller's complex output signal. The original CM cost function is given by

$$J_{pq}^{\mathrm{CM}} = E[|\ \|y(n)\|^p - \delta|^q], \tag{10}$$

where p and q are positive integers and δ is a positive constant related to the constant modulus of the signal constellation. Various adaptive equalizers can be obtained by choosing a (p,q)-variant of the cost function in (10) and the iterative technique for minimizing it with respect to the filter coefficients.

The most famous member of this family of equalizers is the constant modulus algorithm (CMA) for which both parameters p and q are equal to two [20,26]. The CMA attempts to minimize the (2,2)-variant of the cost function shown in (10) by following the path of steepest descent. The adaptation equation is given by

$$\mathbf{w}(n+1) = \mathbf{w}(n) - \mu\mathbf{x}^*(n)\varepsilon(n), \tag{11}$$

$$\varepsilon(n) = y(n)(\|y(n)\|^2 - \delta). \tag{12}$$

Naturally, the shape of the cost surface determines the convergence behavior of a particular stochastic gradient algorithm. The features of the CM cost surface and the associated convergence of the gradient descent algorithm are outlined in a review paper by Johnson et al. [7]. Non-idealities that deform the CM cost surface, causing convergence problems, are due to non-constant modulus and near Gaussian sources, insufficient equalizer length, and additive channel noise. In particular, channel noise squeezes the CM surface minima locations towards the origin and moves further away those being far from the origin. In the following section, we address the effects of additive, possibly heavy-tailed, channel noise to the original CM cost function.

3.2. Introduction to the FLOS-CM criterion

As noted in [7], CMA-based blind equalization is typically successful in moderate noise environments,

i.e., when the signal power is greater than the noise power. It was shown that under modest noise levels, relocation of global minima toward the origin is more severe than changes in surface curvature around such minima. On the other hand, the presence of severe heavy-tailed noise has negative effects on the convergence properties of the CMA, as we demonstrate in Section 4.

By definition (see Eq. (10)), the standard CM cost function ($p = q = 2$) involves fourth-order moments of the measurements. In the presence of heavy-tailed noise, the use of second- or higher-order statistics in effect amplifies the noise. The new criterion that we propose mitigates the noise component by employing fractional lower-order moments of the measurements. The introduced FLOS-CM cost function has the expression

$$J_{p,q}^{\text{FLOS-CM}} = \tfrac{1}{2}E\left[\left|\|y(n)\|^{(p-1)}y(n) - \delta y(n)\right|^{q}\right], \quad (13)$$

where $y(n)$ is the equalizer output and δ is the constant signal modulus to the $p-1$ power. The pair (p,q) takes fractional values between 0 and α, where α is the characteristic exponent of the alpha-stable distribution that best describes the statistics of the additive noise component in $y(n)$. Furthermore, following our discussion in Section 2, the product $p \cdot q$ must be less than α for the FLOS-CM cost function to be well defined, i.e., finite (see (3)).

Two main reasons motivated us in introducing the FLOS-CM cost function. First, under the noise-free hypothesis, the goal of the new criterion should be the restoration of the CM property of the communication signal. In other words, similarly to the original CM algorithm, the FLOS-CM criterion should guarantee that at convergence, $\|y(n)\|^{(p-1)}$ must be equal to the signal constant modulus δ. Second, the new criterion should address the problem of severe channel noise. Indeed, in the presence of heavy-tailed channel noise, the application of fractional lower-order moments (as determined by the use of exponents p and q in the FLOS-CM cost function) to the equalizer output in effect attenuates the noise components. The use of fractional lower-order statistics results to a smooth algorithmic convergence (learning) curve even in the presence of severe channel noise, as we demonstrate in Section 4.

To minimize (13), we use a stochastic gradient descent algorithm that iteratively adjusts the equalizer weights $\mathbf{w}(n)$ as

$$\mathbf{w}(n+1) = \mathbf{w}(n) - \mu\nabla_{\mathbf{w}} J_{p,q}^{\text{FLOS-CM}}, \quad (14)$$

where μ is a small positive step size and $\nabla_{\mathbf{w}}$ is the gradient operator with respect to the elements of the vector $\mathbf{w}$. In practice, the true gradient $\nabla_{\mathbf{w}} J_{p,q}^{\text{FLOS-CM}}$ is replaced by an instantaneous estimate resulting into the so-called FLOS-CM Algorithm (FLOS-CMA). Ignoring the expectation operator and considering the constant modulus δ to be one, the cost function (13) may be re-written as

$$\begin{aligned} J_{p,q} &= \tfrac{1}{2}(y(n)^{(p+1)/2}y(n)^{*(p-1)/2} - y(n))^{q/2} \\ &\quad \times (y(n)^{(p+1)/2}y(n)^{*(p-1)/2} - y(n))^{*q/2} \\ &= \tfrac{1}{2}A(n)^{q/2}(A(n)^{*})^{q/2} \end{aligned} \quad (15)$$

where

$$\begin{aligned} A(n) &= y(n)^{(p+1)/2}y(n)^{*(p-1)/2} - y(n) \\ &= y(n)(\|y(n)\|^{p-1} - 1). \end{aligned} \quad (16)$$

Differentiating (15) in parts, we get that [6]

$$\nabla_{\mathbf{w}} J_{p,q} = 2\frac{\partial J_{p,q}}{\partial \mathbf{w}^{*}} = \frac{\partial A(n)^{q/2}}{\partial \mathbf{w}^{*}}(A(n)^{*})^{q/2} + A(n)^{q/2}\frac{\partial (A(n)^{*})^{q/2}}{\partial \mathbf{w}^{*}}. \quad (17)$$

After some straightforward mathematical manipulation, (17) can be replaced back into (14) to give the FLOS-CMA adaptation:

$$\mathbf{w}(n+1) = \mathbf{w}(n) - \mu\mathbf{x}^{*}(n)\zeta(n), \quad (18)$$

$$\zeta(n) = A(n)\|A(n)\|^{q-2}(p\|y(n)\|^{p-1} - 1). \quad (19)$$

We now turn our attention to the choice of parameters (p,q) in the FLOS-CM cost function. As we have mentioned above, if we are to operate in heavy-tailed noise environments modeled according to a stable law, the main condition that (p,q) must obey is that their product has to be strictly less than α, the characteristic exponent of the alpha-stable channel noise. Hence, any pair of values (p,q) that obeys $pq < \alpha$ gives a well defined cost function. For example, the choice $q = 2$ implies that p should be chosen such that $p < \alpha/2$. The appropriate choice of the FLOS parameters has been extensively studied by the authors in their previous work. Analytical studies,

relating the fractional lower-order power to the degree of data non-Gaussianity (e.g., the parameter α), as well as heuristics have been proposed [15,22,24].

3.3. Lock and capture for the FLOS-CMA

Let us suppose that, in a multipath propagation scenario, all of the transmitted communication signals were originally constant modulus signals. Hence, the question arises how does the FLOS-CMA know which signal to lock onto (capture) and which signals to suppress? Naturally, a solution that nulls all but one of the constant modulus signals corresponds to a stationary point (local minimum) of the FLOS-CM cost function. Intuitively, it is expected that the convergence of the algorithm to a certain stationary point should be a function of relative signal powers and filter initialization. Indeed, in the following, we address the lock and capture properties of the new algorithm by finding the expression of the curve boundaries that divide its convergence regions into positive lock and capture zones.

Part of the analytical difficulty in treating this problem is due to the highly nonlinear form of the FLOS-CM cost function. In this work, we characterize the lock/capture convergence behavior of the proposed FLOS-CMA by considering the case of a noise-free input consisting of only two sinusoids. This model simplifies considerably the mathematical description of the adaptive algorithm and leads to explicit answers to questions regarding its convergence. The simple results provide insight into the problem and can be generalized in the future to accommodate more realistic input signals/noise scenarios, such as multiple tones and modulated communication signals.

We follow a similar approach as in [21] by supposing that the filter input $x(n)$ is given by the sum of two tones with distinct frequencies ω_1 and ω_2

$$x(n) = A_1 e^{j(\omega_1 n+\theta_1)} + A_2 e^{j(\omega_2 n+\theta_2)}, \tag{20}$$

where the amplitudes A_i are real and the phases θ_i are i.i.d. random variables uniformly distributed over the interval $(-\pi,\pi]$. According to (7), it is possible to rewrite the output signal as a function of the two tones

$$y(n) = a_1 A_1 e^{j(\omega_1 n+\theta_1)} + a_2 A_2 e^{j(\omega_2 n+\theta_2)}, \tag{21}$$

where a_1 and a_2 are the complex gains of the adaptive filter at frequencies ω_1 and ω_2, respectively. If we define the frequency steering vector $\mathbf{v}(\omega)$ to be

$$\mathbf{v}(\omega) = [1 e^{j\omega} \cdots e^{j\omega(N-1)}]^t \tag{22}$$

then each complex gain a_i may be expressed as

$$a_i = \mathbf{v}^H(\omega_i)\mathbf{w}. \tag{23}$$

With no loss of generality, we assume the signal at frequency ω_1 to be the signal of interest. Hence, the desired filter output is reached when $|a_1|A_1 = 1$ and $|a_2|A_2 = 0$.

As described in [21], we proceed by finding a compact form that compresses the adaptive weight recursion of (18) into a two-by-two recursion on the tone output amplitudes a_1 and a_2. For ease of mathematical analysis, we consider the $(p,2)$-variant of the FLOS-CMA. By taking expectations on both sides of (18) and by using the independence assumption commonly employed in the analysis of adaptive algorithms, the ensemble average of the weight vector, $\mathbf{w}(n)$, can be written as

$$E[\mathbf{w}(n+1)] = \{\mathbf{I} - \mu\mathbf{H}(n)\}E[\mathbf{w}(n)], \tag{24}$$

where

$$\mathbf{H}(n) = E[(p\|y(n)\|^{2(p-1)} - (p+1) \times \|y(n)\|^{p-1} + 1)\mathbf{x}^*(n)\mathbf{x}^t(n)]. \tag{25}$$

The independence hypothesis is reasonably good if the step size is small so as to consider $\mathbf{H}(n)$ to be uncorrelated with $\mathbf{w}(n)$. The (l,r) element of $\mathbf{H}(n)$ is given by

$$H_{l,r} = E[(p\|y(n)\|^{2(p-1)} - (p+1) \times \|y(n)\|^{p-1} + 1)x^*(n-l)x(n-r)]. \tag{26}$$

Since (26) contains fractional lower-order powers of $y(n)$, we have to use the *Generalized Binomial Theorem*, which is valid for real exponent values [4] and it allows us to expand the individual contributions as the sum of finite fractional power terms. Furthermore, recalling that θ_1 and θ_2 are i.i.d. random variables over the interval $(-\pi,\pi]$, the expectation of all the elements in the series that contain some power of θ_i is equal to zero for $i = 1,2$. Finally, we obtain

$$H_{l,r} = (pP^{p-1} - (1+p)P^{(p-1)/2} + 1) \times (A_1^2 e^{j(l-r)\omega_1} + A_2^2 e^{j(l-r)\omega_2})$$

$$+\left(p(p-1)P^{p-2} -(1+p)\frac{p-1}{2}P^{((p-1)/2)-1}\right) \times A_1^2A_2^2\left(a_1a_2^*e^{j(l\omega_1-r\omega_2)}+a_1^*a_2e^{j(l\omega_2-r\omega_1)}\right), \quad (27)$$

$$P=A_1^2\|a_1\|^2+A_2^2\|a_2\|^2. \quad (28)$$

As the only non-zero terms are the ones independent from θ_1,θ_2 we can now write the recursive equation (18) as

$$E[\mathbf{w}(n+1)]=\{\mathbf{I}-\mu\mathbf{V}\mathbf{Q}\mathbf{V}^H\}E[\mathbf{w}(n)], \quad (29)$$

where the matrix $\mathbf{V}=[\mathbf{v}(\omega_1)\,\mathbf{v}(\omega_2)]$ is formed by the steering vectors at the tone frequencies and the elements of the 2×2 matrix $\mathbf{Q}$ are given by

$$q_{1,1}=A_1^2(P^{p-1}-(1+p)P^{(p-1)/2}+1), \quad (30)$$

$$q_{1,2}=A_1^2A_2^2\left(p(p-1)P^{p-2}-(1+p)\times\frac{p-1}{2}P^{((p-1)/2)-1}\right)a_1a_2^*, \quad (31)$$

$$q_{2,1}=A_1^2A_2^2\left(p(p-1)P^{p-2}-(1+p)\times\frac{p-1}{2}P^{((p-1)/2)-1}\right)a_1^*a_2, \quad (32)$$

$$q_{2,2}=A_2^2(P^{p-1}-(1+p)P^{(p-1)/2}+1). \quad (33)$$

Since the weight vector $\mathbf{w}(n)$ is adapted with time, the complex gains a_i will also be updated. Assuming that the steering vectors, which correspond to the two sources, are orthogonal to each other, it holds that

$$\mathbf{v}^H(\omega_0)\mathbf{v}(\omega_0)=N \quad \text{and} \quad \mathbf{v}^H(\omega_0)\mathbf{v}(\omega_1)=0. \quad (34)$$

In this case, by combining (23), (29), and (34), we can get a recursion on the two-dimensional vector of complex gains $\mathbf{a}(n)=[a_1(n)\,a_2(n)]^t$:

$$\mathbf{a}(n+1)=[\mathbf{I}-\mu N\mathbf{Q}]\mathbf{a}(n). \quad (35)$$

If we then define the complex output amplitudes, $b_1(n)=A_1a_1(n)$ and $b_2(n)=A_2a_2(n)$, as the input amplitudes scaled by the instantaneous filter gain at the corresponding frequency, we get that

$$b_1(n+1)=\left[1-\mu N|A_1|^2(pP^{(p-2)}(|b_1(n)|^2+p|b_2(n)|^2) -\left((1+p)P^{((p-1)/2-1)}\left(|b_1(n)|^2+\left(\frac{p+1}{2}\right)|b_2(n)|^2\right)+1\right)\right]b_1(n), \quad (36)$$

$$b_2(n+1)=\left[1-\mu N|A_2|^2(pP^{(p-2)}(p|b_1(n)|^2+|b_2(n)|^2) -\left((1+p)P^{((p-1)/2-1)}\left(\left(\frac{p+1}{2}\right)|b_1(n)|^2+|b_2(n)|^2\right)+1\right)\right]b_2(n). \quad (37)$$

A close examination of Eqs. (36) and (37) reveals that, although we would like the two gains $b_1(n)$ and $b_2(n)$ to be decoupled, they are still linked by the nonlinear crossterms in the transition coefficients. These expressions are similar to analogous expressions that were derived for the CMA in [21]. For the proposed criterion though, fractional lower-order powers appear instead of just square powers.

Even so, the two-dimensional model (36) and (37) allows us to describe the capture and lock behavior of FLOS-CMA. Starting with the amplitude of $b_1(n)$, we have that

$$|b_1(n+1)|=|b_1(n)|\,|1-\mu N|A_1|^2\left[pP^{(p-2)}(|b_1(n)|^2+p|b_2(n)|^2)-(1+p)P^{((p-1)/2-1)}\left(|b_1(n)|^2+\frac{p+1}{2}|b_2(n)|^2\right)+1\right]|. \quad (38)$$

Assuming that μ is small enough so that

$$|\mu N|A_1|^2\left\{pP^{(p-2)}(|b_1(n)|^2+p|b_2(n)|^2)-(1+p)\times P^{((p-1)/2-1)}\left(|b_1(n)|^2+\left(\frac{p+1}{2}\right)|b_2(n)|^2\right)+1\right\}|\ll 1 \quad (39)$$

it is possible to find the conditions for which $|b_1(n)|$ increases (i.e., $|b_1(n+1)|>|b_1(n)|$) or decreases

(i.e., $|b_1(n+1)| < |b_1(n)|$ with time:

$$1 + pP^{(p-2)}(|b_1(n)|^2 + p|b_2(n)|^2) - (1+p)P^{((p-1)/2-1)} \times \left(|b_1(n)|^2 + \left(\frac{p+1}{2}\right)|b_2(n)|^2\right) \begin{cases} > 0 & |b_1(n)| \text{ decays}, \\ < 0 & |b_1(n)| \text{ grows}. \end{cases} \quad (40)$$

Using similar arguments, the convergence behavior of the second tone is determined by

$$1 + pP^{(p-2)}(p|b_1(n)|^2 + |b_2(n)|^2) - (1+p)P^{((p-1)/2-1)} \left(\left(\frac{p+1}{2}\right)|b_1(n)|^2 + |b_2(n)|^2\right) \begin{cases} > 0 & |b_2(n)| \text{ decays}, \\ < 0 & |b_2(n)| \text{ grows}. \end{cases} \quad (41)$$

Expressions (40) and (41) define the growth and decay of the two gains. A graphic description of the two conditions divides the $(|b_1|, |b_2|)$ space to regions of so-called "positive lock" and "positive capture" that are shown in Fig. 3. The curve bounds, depicted in the figure, are obtained by setting (40) and (41) equal to zero. The desired lock condition occurs when $|b_1| = 1$ and $|b_2| = 0$, i.e., the tone of interest is filtered by the adaptive equalizer with unit amplitude while the interfering tone is totally suppressed. If the algorithm is initialized in the positive lock region, then $|b_1|$ will converge towards 1 while $|b_2|$ will ultimately decay to zero. On the other hand, if initialized in the positive lock region, the FLOS-CMA will converge to the point $(|b_1| = 0, |b_2| = 1)$ and interference capture will occur.

Comparing Fig. 3, with an analogous figure in [21] that depicts the lock/capture behavior of the original CMA, one observes that the introduced FLOS-CM cost function produces a new "zero capture" region near the origin. When the algorithm is initialized in this region, $|b_1|$ and $|b_2|$ will be constrained to decay to zero, i.e., both tones will be suppressed. For this

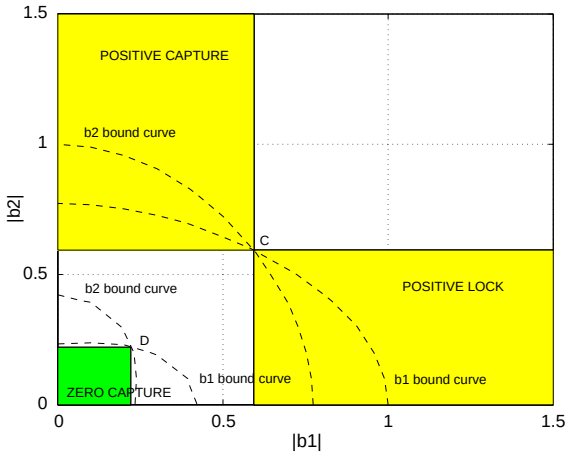

Fig. 3. FLOS-CMA: Positive lock, positive capture, and zero capture regions.

reason, we need to set the initial weights to provide an output coordinate away for the zero capture area. In general, erroneous convergence to zero or interference capture can be avoided with proper initialization of the adaptive algorithm into the positive lock region. Capture avoidance guidelines are given in [21] when provided with (i) a priori estimates of the desired tone amplitude and frequency, (ii) amplitude but no frequency estimates of both components, and (iii) dynamic environments where an interferer may suddenly appear. Eq. (39) and the analogous equation obtained for the second source b_2

$$|\mu N|A_2|^2 \left\{ pP^{(p-2)}[p|b_1(n)|^2 + |b_2(n)|^2] - (1+p) \times P^{((p-1)/2-1)} \left[\left(\frac{p+1}{2}\right)|b_1(n)|^2 + |b_2(n)|^2\right] + 1 \right\} | \ll 1 \quad (42)$$

can give a criterion for choosing the step size as the minimum μ value between (39) and (42).

It is of interest to predict the FLOS-CMA behavior in the remaining (non-shadowed) regions in Fig. 3. To achieve that, we express the slope of the adaptation trajectory as a function of the signal-to-interference ratio (SIR). First, consider the intersection points C and D of the curve bounds in Fig. 3. Their coordinates, obtained by equating (40) and (41),

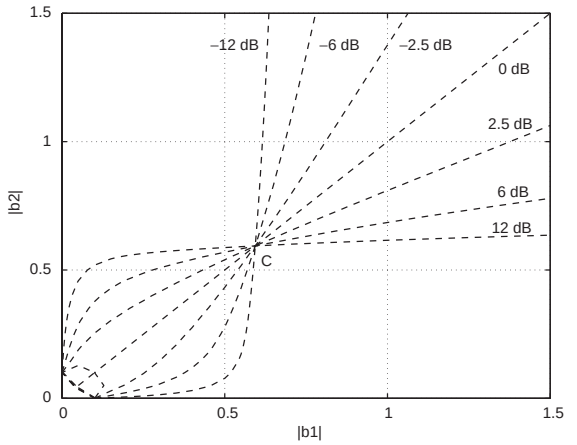

Fig. 4. FLOS-CMA: Lock and capture boundaries as a function of signal-to-interference ratio.

are given by

$$b_{C,D} = \left[\frac{(1+p)2^{((p-5)/2)}(p+3) \pm \sqrt{((1+p)2^{((p-5)/2)}(p+3))^2 - 4p(1+p)2^{(p-2)}}}{2p(1+p)2^{(p-2)}} \right]^{1/(p-1)}. \quad (43)$$

The intersection point C between the lock/capture regions corresponds to the positive sign of the square root in (43). We can define the borderline between capture and lock as the trajectory that leads to point C. This trajectory curve is obtained by setting the slope between operational points at times n and $n+1$ to be equal to the critical slope between the point at time n and point C:

$$\frac{b_1(n) - b_C}{b_2(n) - b_C} = \frac{b_1(n+1) - b_1(n)}{b_2(n+1) - b_2(n)}. \quad (44)$$

Using (36) to (41), and defining SIR to be $SIR = A_1^2/A_2^2$, we obtain the border loci

$$\mathrm{SIR} = \frac{(|b_1(n)| - b_C)(pP^{(p-2)}b_{1p,2} - (1+p)P^{(((p-1)/2)-1)}b_{1((p+1)/2,2} + 1)|b_2(n)|}{(|b_2(n)| - b_C)(pP^{(p-2)}b_{1,2p} - (1+p)P^{(((p-1)/2)-1)}b_{1,2((p+1)/2} + 1)|b_1(n)|}, \quad (45)$$

$$b_{1p,2} = p|b_1(n)|^2 + |b_2(n)|^2, \quad (46)$$

$$b_{1,2p} = |b_1(n)|^2 + p|b_2(n)|^2, \quad (47)$$

$$b_{1((p+1)/2,2} = \left(\frac{p+1}{2}\right)|b_1(n)|^2 + |b_2(n)|^2, \quad (48)$$

$$b_{1,2((p+1)/2} = |b_1(n)|^2 + \left(\frac{p+1}{2}\right)|b_2(n)|^2. \quad (49)$$

Various such trajectories described by (45) are plotted in Fig. 4 for different SIR values. It is clear that, for a certain SIR, initialization of the FLOS-CMA below and to the right of the trajectory results to lock of the signal of interest at convergence. Here also, the difference with the original CMA behavior is due to the existence of the zero capture region near the origin. Initialization near that region will trap the solution near zero, far from the signal of interest or the interference.

4. Simulation results

In this section, we test the new FLOS-CM adaptive algorithm and compare its performance with that of the conventional CMA in various noise environments and by using two source constellations, a $\pi/4$ QPSK CM signal and a 16-QAM nonconstant modulus alphabet. Since the success of any stochastic gradient descent equalizer adaptation algorithm is dependent on a certain degree of stationarity in the received process, in our set of simulations, we restrict our focus to stationary source and noise processes and to channels whose impulse response is fixed. We work with baud-spaced equalizer coefficient vectors, although fractionally spaced channel equalization can be implemented and tested in a straightforward manner [7]. Another point of interest relates to the fact that the FLOS-CM (like the original CM) cost surface is unavoidably multimodal. Hence, the choice of initialization affects both the convergence time and the steady-state performance of the algorithm. Here, we follow the approach suggested in [7] and we initialize the equalizer with a single spike, time-aligned with the channel response's center of mass. In this way, crude knowledge of the channel impulse response envelope can be used to aid initialization.

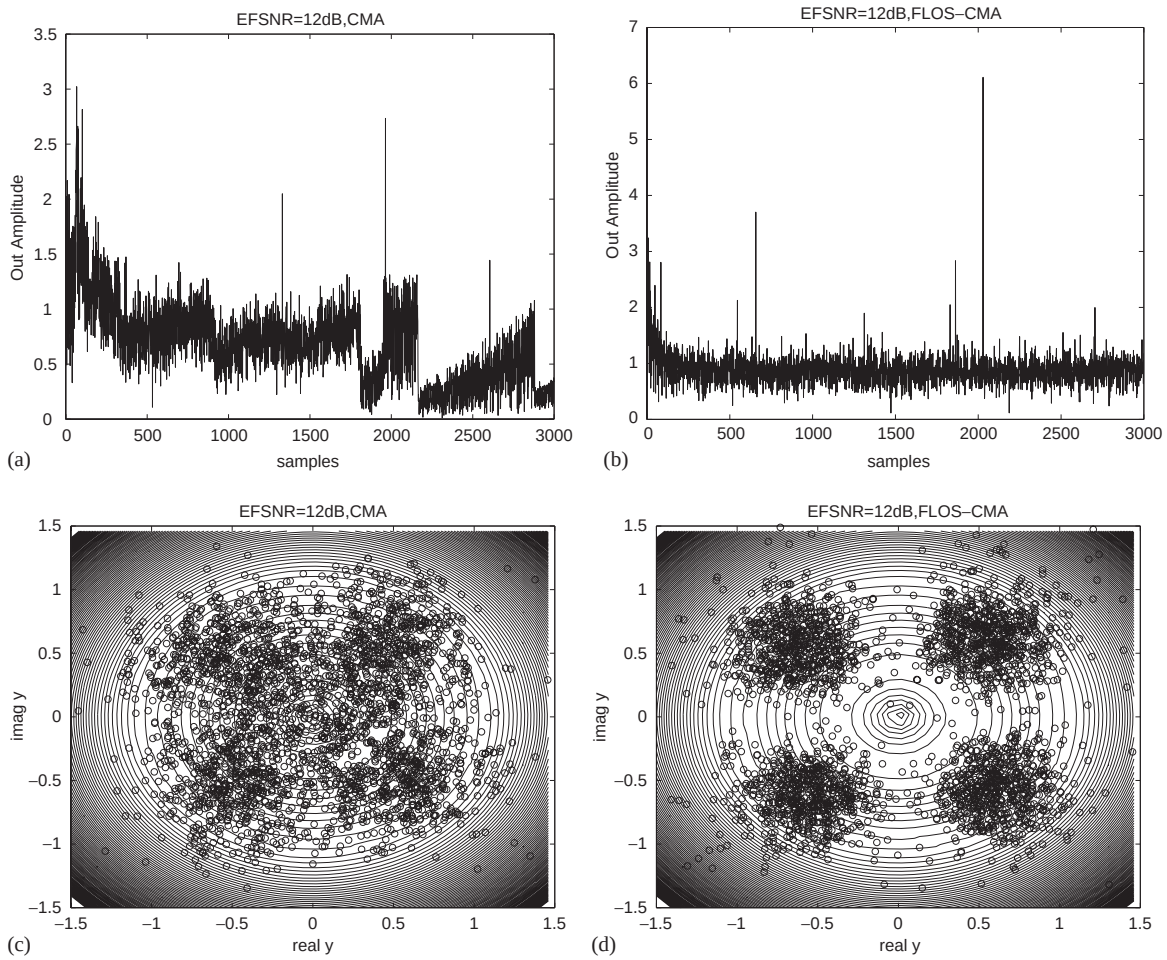

Fig. 5. Amplitude output of the CMA (a) and FLOS-CMA (b). Signal constellation pattern of equalizer output for the CMA (c) and FLOS-CMA (d). A $\pi/4$ QPSK CM input signal is passed through a two-tap channel. Additive $S\alpha S$ noise is present with $\alpha = 1.85$ and EFSNR $= 12$ dB.

We use the $S\alpha S$ model to describe the additive noise component. We should note here that although the moment $E[|X|^2]$ of a second-order process is widely accepted as a standard measure of signal strength and associated with the physical concept of power and energy, it cannot be used with alpha-stable distributions because it is infinite. In our simulations, we define the *effective fractional SNR* (EFSNR) to be the ratio of the fractional signal power of α over the fractional noise power of α:

$$\text{EFSNR} = \sum_{k=1}^{M} \frac{|\mathbf{s}(k)|^{\alpha}}{|\mathbf{n}(k)|^{\alpha}}. \tag{50}$$

Initially, the $\pi/4$ QPSK CM signal is passed through a two-tap channel with coefficients [1 0.5]. The resulting two paths are observed at the receiver in the presence of alpha-stable noise with characteristic exponent $\alpha = 1.85$ and a EFSNR equal to 12 dB. We should note that values of α in ranges around 1.8 have been observed in the modeling of real data. For example, Stuck and Kleiner empirically found that the noise over certain telephone lines can be best described by a $S\alpha S$ model with $\alpha \approx 1.87$ [19] while Tsakalides and Nikias have used $S\alpha S$ densities with $\alpha \approx 1.74$ to model actual sea clutter data [23]. This choice of α corresponds to a noise process with a moderate degree of

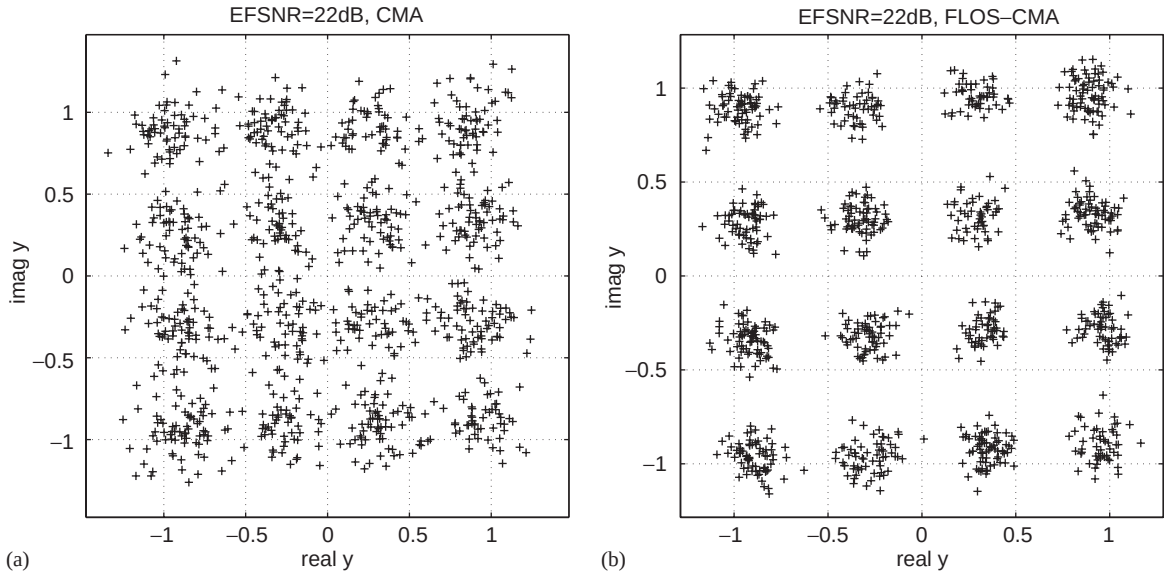

Fig. 6. Signal constellation pattern of equalizer output for the CMA (a) and FLOS-CMA (b). A 16-QAM non-CM input signal is passed through a four-tap channel. Additive $S\alpha S$ noise is present with $\alpha = 1.85$ and EFSNR = 22 dB.

non-Gaussianity. To recover the communication signal, we designed an eight-tap adaptive equalizer based on the CM and FLOS-CM criteria. In the simulations, we chose the FLOS-CMA step size according to (39) and (42) and the CMA stepsize according to guidelines described in [21].

Fig. 5 depicts the output amplitude of the CM (5(a)) and FLOS-CM ($(p,q) = (1.1, 1.3)$) (5(b)) filters as a function of time (iteration samples). It is apparent that the FLOS-CMA has a smoother convergence behavior than the CMA. The figure demonstrates that occurrences of noise outliers during the adaptation procedure have an adverse affect to the learning curve of the original CMA but do not affect as much the proposed FLOS-CMA. Fig. 5 also demonstrates that the associated received vectors of the adapted FLOS-CMA method are tightly clustered about the four constellation points (Fig. 5(d)), while the signal constellation of the original CMA is not as well defined (Fig. 5(c)).

The issue of the performance of CMA-variants in the presence of non-CM source alphabets is unavoidable in communication systems using multilevel constellations. Extensive studies in the literature point to the fact that non-CM sources tend to raise and flatten the CM surface (as a consequence of increased source kurtosis) but do not alter the minima locations [7]. In our simulations, we also test the FLOS-CMA by using a 16-QAM non-CM signal that is passed through a four-tap channel with coefficients [0.2 0.5 1 -0.1]. Additive alpha-stable noise with characteristic exponent $\alpha = 1.85$ is present with an EFSNR equal to 22 dB. Fig. 6 illustrates that both CMA and FLOS-CMA are efficient with non-CM signals, although again, for this type of non-Gaussian noise, FLOS-CMA results in signals more tightly clustered about the 16 constellation points.

It should be expected that the performance improvement achieved with the FLOS-CM processing is related to the degree of non-Gaussianity of the additive noise. To quantify the above illustrative results, we calculated the bit error rate (BER) versus the EFSNR for the original CMA and the proposed FLOS-CMA in the presence of Gaussian noise ($\alpha = 2$) and $S\alpha S$ noise with $\alpha = 1.85$. The resulting curves correspond to the $\pi/4$ QPSK CM signal and the two-tap channel model. Fig. 7 demonstrates that the BER performance of the two methods is comparable for Gaussian environments, with the original CMA holding a slight edge. But when the noise deviates from Gaussianity, the proposed FLOS-CMA has a robust performance

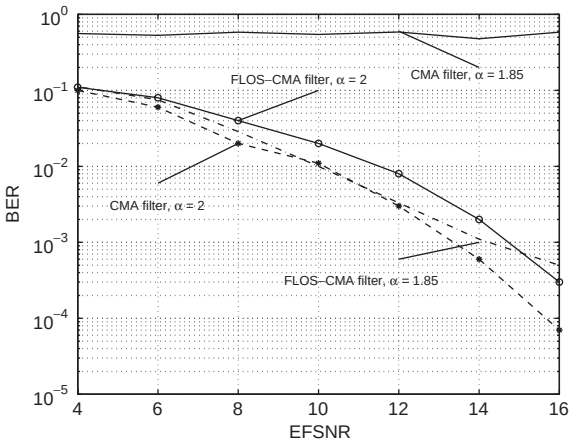

Fig. 7. Bit error rate (BER) versus effective fractional signal-to-noise ratio for the CM and FLOS-CM equalizers in Gaussian ($\alpha = 2$) and $S\alpha S$ noise with $\alpha = 1.85$. The curves correspond to the $\pi/4$ QPSK input signal and the two-tap channel model.

while the BER of the original CMA increases to unacceptably high levels.

5. Conclusions

We proposed a new method for blind equalization of communication signals using a constant modulus criterion based on fractional lower-order statistics. The introduced FLOS-CM filter exploits the constant modulus property of the signal of interest to compensate for the fading and multipath effects of a communication channel. At the same time, it uses the heavy-tailed noise suppression capabilities of FLOS to mitigate the channel additive noise component. The main advantage of the proposed method is its robustness in the presence of various noise environments. Truly, by changing the parameters p and q in the cost function we may obtain a class of FLOS-based CMA filters, which provides considerable flexibility that can be useful for optimization purposes in the presence of non-stationary noise environments.

The proposed method developed using FLOS has approximately the same computational complexity as the existing CM methods. The additional computational load is due to the need for calculating a fractional power ($p < 2$) rather than a square power. The technique can be used in commercial communication applications in which impulsive channels tend to produce large-amplitude interferences and sharp noise spikes more frequently than what is expected from Gaussian channels.

Acknowledgements

The work of the second author was supported by the Greek General Secretariat for Research and Technology under Programs EPET II, Code 97EL-152 and EPAN, Code USA-011.

References

[1] R. Adler, R. Feldman, M.S. Taqqu, A Practical Guide to Heavy Tails: Statistical Techniques and Applications, Birkhauser, Boston, MA, 1998.
[2] M.E. Crovella, M.S. Taqqu, A. Bestavros, Heavy-tailed probability distributions in the World Wide Web, in: R. Adler, R. Feldman, M.S. Taqqu (Eds.), A Practical Guide to Heavy Tails: Statistical Techniques and Applications, Birkhauser, Boston, 1998, pp. 3–25.
[3] I. Fijalkow, A. Touzni, J. Treichler, Fractionally spaced equalization using cma: robustness to channel noise and lack of disparity, IEEE Trans. Signal Proc. 45 (January 1997) 56–66.
[4] E. Giusti, Analisi matematica, 2. Editore Boringhieri, 1988.
[5] D.N. Godard, Self-recovering equalization and carrier tracking in a two-dimensional data communication system, IEEE Trans. Commun. 28 (August 1980) 1867–1875.
[6] S. Haykin, Adaptive Filter Theory, 3rd Edition, Prentice-Hall, Englewood Cliffs, NJ, 1996.
[7] C.R. Johnson, P. Schniter, T.J. Endres, J.D. Behm, D.R. Brown, R.A. Casas, Blind equalization using the constant modulus criterion: a review, Proc. IEEE 86 (October 1998) 1927–1950.
[8] S.A. Kassam, H.V. Poor, Robust techniques for signal processing: a survey, Proc. IEEE 73 (March 1985) 433–481.
[9] D. Middleton, Statistical-physical models of urban radio noise environment—Part i: foundations, IEEE Trans. Elect. Comput. 14 (January 1972) 38–56.
[10] U. Mitra, H. Poor, Detection of spread-spectrum signals in multi-user environment, in: Proceedings of IEEE ICASSP, Detroit, Michigan, May 9–12, 1995, pp. 1844–1847.
[11] C.L. Nikias, M. Shao, Signal Processing with Alpha-Stable Distributions and Applications, Wiley, New York, 1995.
[12] J. Proakis, Digital Communications, McGraw-Hill, New York, 1995.
[13] C.L. Nikias, I.S. Reed, V. Prasanna, Multidisciplinary research on advanced high-speed, adaptive signal processing for radar sensor, Technical Report, University of Southern California, June 1996.

[14] M. Rupi, P. Tsakalides, C.L. Nikias, E. Del Re, Robust constant modulus arrays based on fractional lower-order statistics, IEEE ICASSP, Phoenix, 15–19 March 1999, pp. 2945–2948.
[15] M. Rupi, P. Tsakalides, E.D. Re, C.L. Nikias, Robust spatial filtering of coherent sources for wireless communications, Signal Processing 80 (March 2000) 381–396.
[16] Y. Sato, A method of self-recovering equalization for multilevel-amplitude modulation systems, IEEE Trans. Commun. 23 (June 1975) 679–682.
[17] M. Schilder, Some structure theorems for the symmetric stable laws, The Ann. Math. Statist. 41 (1970) 412–421.
[18] B.W. Stuck, B. Kleiner, A statistical analysis of telephone noise, Technical Report, Bell. Syst. Tech. J., June 1974.
[19] B.W. Stuck, B. Kleiner, A statistical analysis of telephone noise, Bell Syst. Tech. J. 53 (1974) 1263–1320.
[20] J. Treichler, M. Larimore, New processing techniques based on the constant modulus adaptive algorithm, IEEE Trans. Acoust. Speech Signal Process. 33 (2) (April 1985) 420–431.
[21] J. Treichler, M. Larimore, The tone capture properties of cma-based interference suppressors, IEEE Trans. Acoust. Speech Signal Process. 33 (August 1985) 946–958.
[22] P. Tsakalides, C.L. Nikias, The robust covariation-based MUSIC (ROC-MUSIC) algorithm for bearing estimation in impulsive noise environments, IEEE Trans. Signal Process. 44 (July 1996) 1623–1633.
[23] P. Tsakalides, C.L. Nikias, The robust covariation-based MUSIC (ROC-MUSIC) algorithm for bearing estimation in impulsive noise environments, IEEE Trans. Signal Process. 44 (July 1996) 1623–1633.
[24] P. Tsakalides, C.L. Nikias, High resolution autofocus techniques for SAR imaging based on fractional lower-order statistics, IEE Proc.-Radar Sonar and Navigation 148(5) (October 2001) 267–276.
[25] X. Wang, H.V. Poor, Robust multiuser detection in non-Gaussian channels, IEEE Trans. Signal Process. 47 (February 1999) 289–305.
[26] J.R. Treichler, B.G. Agee, A new approach to multipath correction of constant modulus signals, IEEE Trans. Acoust. Speech Signal Process. 31 (April 1983) 459–471.